

¹ cortecs: A Python package for compressing opacities

² Arjun B. Savel  ^{1,2}, Megan Bedell  ², and Eliza M.-R. Kempton  ¹

³ 1 Astronomy Department, University of Maryland, College Park, 4296 Stadium Dr., College Park, MD

⁴ 207842 USA 2 Flatiron Institute, Simons Foundation, 162 Fifth Avenue, New York, NY 10010, USA 

⁵ Corresponding author

DOI: [10.xxxxxx/draft](https://doi.org/10.xxxxxx/draft)

Software

- [Review](#) 
- [Repository](#) 
- [Archive](#) 

Editor: Ivelina Momcheva  

Reviewers:

- [@pscicluna](#)
- [@doriannblain](#)

Submitted: 03 November 2023

Published: unpublished

License

Authors of papers retain copyright and release the work under a Creative Commons Attribution 4.0 International License ([CC BY 4.0](#))

⁶ Summary

⁷ The absorption and emission of light by exoplanet atmospheres encode details of atmospheric composition, temperature, and dynamics. Fundamentally, simulating these processes requires detailed knowledge of the opacity of gases within an atmosphere. When modeling broad wavelength ranges at high resolution, such opacity data for even a single gas can take up multiple gigabytes of system random-access memory (RAM). This aspect can be a limiting factor in determining the number of gases to consider in a simulation, or even in choosing the architecture of the system used for the simulation. Here, we present cortecs, a Python tool for compressing opacity data. cortecs provides flexible methods for fitting the temperature, pressure, and wavelength dependencies of opacity data and for evaluating the opacity with accelerated, GPU-friendly methods. The package is actively developed on GitHub (<https://github.com/arjunsavel/cortecs>), and it is available for download with pip.

¹⁸ Statement of need

²⁰ Observations with the latest high-resolution spectrographs (e.g., [Mace et al., 2018](#); [Pepe et al., 2021](#); [Seifahrt et al., 2020](#)) have motivated RAM-intensive simulations of exoplanet atmospheres at high spectral resolution. cortecs enables these simulations with more gases and on a broader range of computing architectures by compressing opacity data.

²² Broadly, generating a spectrum to compare against recent high-resolution data requires solving the radiative transfer equation over tens of thousands of wavelength points ([Beltz et al., 2023](#); [Gandhi et al., 2023](#); [Line et al., 2021](#); [Maguire et al., 2023](#); [Prinot et al., 2023](#); e.g., [Savel et al., 2022](#); [Wardenier et al., 2023](#)). To decrease computational runtime, some codes have parallelized the problem on GPUs ([Lee et al., 2022](#); e.g., [Line et al., 2021](#)). However, GPUs cannot in general hold large amounts of data in their video random-access memory (VRAM) (e.g., [Ito et al., 2017](#)); only the cutting-edge, most expensive GPUs are equipped with VRAM in excess of 30 GB (such as the NVIDIA A100 or H100). RAM and VRAM management is therefore a clear concern when producing high-resolution spectra.

³² How do we decrease the RAM footprint of these calculations? By far the largest contributor to the RAM footprint, at least as measured on disk, is the opacity data. For instance, the opacity data for a single gas species across the wavelength range of the Immersion GRating INfrared Spectrometer spectrograph [IGRINS; [Mace et al. \(2018\)](#)] takes up 2.5 GB of non-volatile memory (i.e., the file size is 2.5 GB) at float64 precision and at a resolving power of 400,000 (as used in ([Line et al., 2021](#)), with 39 temperature points and 18 pressure points, using, e.g., the ([Polyansky et al., 2018](#)) water opacity tables). It stands to reason that decreasing the amount of RAM/VRAM consumed by opacity data would strongly decrease the total amount of RAM/VRAM consumed by the radiative transfer calculation.

⁴¹ One solution is to isolate redundancy: While the wavelength dependence of opacity is sharp

42 for many gases, the temperature and pressure dependencies are generally smooth and similar
43 across wavelengths (e.g., Barber et al., 2014; Coles et al., 2019; Polyansky et al., 2018). This
44 feature implies that the opacity data should be compressible without significant loss of accuracy
45 at the spectrum level.

46 While our benchmark case (see Benchmark) demonstrates the applicability of cortecs to
47 high-resolution opacity functions of molecular gas, the package is general and can be applied
48 to any opacity data that has pressure and temperature dependence, such as the opacity of
49 neutral atoms or ions. Additionally, the code has only been verified to produce reasonable
50 amounts of error in the spectra of exoplanet atmospheres at pressures greater than a microbar
51 for a single composition. This caveat is important to note for a few reasons:

- 52 1. Based on error propagation, the error in the opacity function will be magnified in the
53 spectrum based on the number of cells that are traced during radiative transfer. The
54 number of spatial cells used to simulate exoplanet atmospheres (in our case, 100) is
55 small enough that the cortecs error is not massive at the spectrum level.
- 56 2. Exoplanet atmospheres can justifiably be modeled as in hydrostatic equilibrium at
57 pressures greater than a microbar. When modeling atmospheres in hydrostatic equilibrium,
58 the final spectrum essentially maps to the altitude at which the gas becomes optically
59 thick. If cortecs-compressed opacities were used to model an optically thin gas over
60 large path lengths, then smaller opacities would be more important. However, cortecs
61 tends to perform worse at modeling opacity functions that jump from very low to very
62 high opacities, so it may not perform optimally for these optically thin scenarios.
- 63 3. The program may perform poorly for opacity functions with sharp features in their
64 temperature–pressure dependence. That is, it may require so many parameters to fit the
65 opacity function that the compression is no longer worthwhile.

66 Methods

67 cortecs seeks to compress redundant information by representing opacity data not as the
68 opacity itself but as fits to the opacity as a function of temperature and pressure. We generally
69 refer to this process as “compression” as opposed to “fitting” to emphasize that we do not
70 seek to construct physically motivated, predictive, or comprehensible models of the opacity
71 function. Rather, we simply seek representations of the opacity function that consume less
72 RAM/VRAM. The compression methods we use are “lossy”—the original opacity data
73 cannot be exactly recovered with our methods. We find that the loss of accuracy is tolerable
74 for at least the hot Jupiter emission spectroscopy application (see Benchmark below).

75 We provide three methods of increasing complexity (and flexibility) for compressing and
76 decompressing opacity: polynomial-fitting, principal components analysis (PCA, e.g., Jolliffe &
77 Cadima, 2016) and neural networks (e.g., Alzubaidi et al., 2021). The default neural network
78 architecture is a fully connected neural network; the user can specify the desired hyperparameters,
79 such as number of layers, neurons per layer, and activation function. Alternatively, any keras
80 (Chollet & others, 2015) model can be passed to the fitter. Each compression method is paired
81 with a decompression method for evaluating opacity as a function of temperature, pressure,
82 and wavelength. These decompression methods are tailored for GPUs and are accelerated
83 with the JAX code transformation framework (Bradbury et al., 2018). An example of this
84 reconstruction is shown in Figure 1.

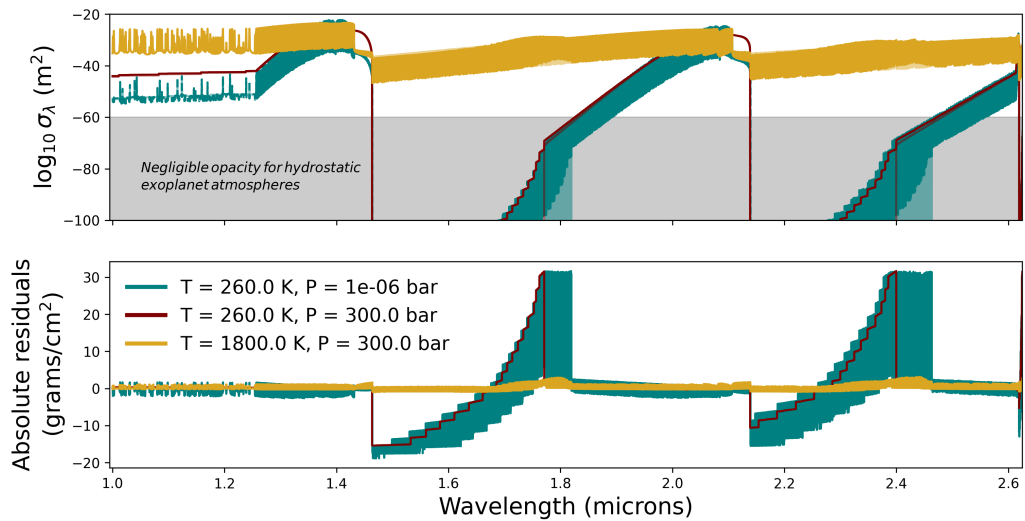


Figure 1: Top panel: The original opacity function of CO (Rothman et al., 2010) (solid lines) and its cortecs reconstruction (transparent lines) over a large wavelength range and at multiple temperatures and pressures. Bottom panel: the absolute residuals between the opacity function and its cortecs reconstruction. Note that opacities less than 10^{-60} are not generally relevant for the benchmark presented here; an opacity of $\sigma_\lambda = 10^{-60}$ would require a column nearly 10^{27} m long to become optically thick at a pressure of 1 bar and temperature of 1000 K.

85 Workflow

86 A typical workflow with cortecs involves the following steps:

- 87 1. Acquiring: Download opacity data from a source such as the ExoMol database (Tennyson
88 et al., 2016) or the HITRAN database (Gordon et al., 2017).
- 89 2. Fitting: Compress the opacity data with cortecs's fit methods.
- 90 3. Saving: Save the compressed opacity data (the fitted parameters) to disk.
- 91 4. Loading: Load the compressed opacity data from disk in whatever program you're
92 applying the data—e.g., within your radiative transfer code.
- 93 5. Decompression: Evaluate the opacity with cortecs's eval methods.

94 The accuracy of these fits may or may not be suitable for a given application. It is important to
95 test that the error incurred using cortecs does not impact the results of your application—for
96 instance, by using the cortecs.fit.metrics.calc_metrics function to calculate the error
97 incurred by the compression and by calculating spectra with and without using cortecs-
98 compressed opacities. We provide an example of such a benchmarking exercise below.

99 Benchmark: High-resolution retrieval of WASP-77Ab

100 As a proof of concept, we perform a parameter inference exercise (a “retrieval,” Madhusudhan
101 & Seager, 2009) on the high-resolution thermal emission spectrum of the fiducial hot Jupiter
102 WASP-77Ab (August et al., 2023; Line et al., 2021; Mansfield et al., 2022) as observed at
103 IGRINS. The retrieval pairs PyMultiNest (Buchner et al., 2014) sampling with the CHIMERA
104 radiative transfer code (Line et al., 2013), with opacity from H₂O (Polyansky et al., 2018),
105 CO (Rothman et al., 2010), CH₄ (Hargreaves et al., 2020), NH₃ (Coles et al., 2019), HCN
106 (Barber et al., 2014), H₂S (Azzam et al., 2016), and H₂ – H₂ collision-induced absorption
107 (Karman et al., 2019). The non-compressed retrieval uses the data and retrieval framework
108 from (Line et al., 2021), run in an upcoming article (Savel et al. 2024, submitted). For this
109 experiment, we use the PCA-based compression scheme implemented in cortecs, preserving 3

110 principal components and their corresponding weights as a function for each wavelength as a
111 lossy compression of the original opacity data.

112 Using cortecs, we compress the input opacity files by a factor of 13. These opacity data (cite
113 them) were originally stored as 2.0 GB .h5 files containing 39 temperature points, 18 pressure
114 points, and 373,260 wavelength points. The compressed opacity data are stored as 154 MB
115 files of PCA coefficients and 1.1 KB files of PCA vectors (which are reused for each wavelength
116 point). These on-disk memory quotes are relatively faithful to the in-memory RAM footprint
117 of the data when stored as numpy arrays (2.1 GB for the uncompressed data and 160 MB for
118 the compressed data). Reading in the original files takes 1.1 ± 0.1 seconds, while reading in
119 the compressed files takes 24.4 ± 0.3 ms. Accessing/evaluating an opacity value takes 174.0
120 ± 0.5 ns for the uncompressed data and 789 ± 5 ns for the compressed data. All of these
121 timing experiments are performed on a 2021 MacBook Pro with an Apple M1 Pro chip and 16
122 GB of RAM.

123 Importantly, we find that our compressed-opacity retrieval yields posterior distributions (as
124 plotted by the corner package, [Foreman-Mackey, 2016](#)) and Bayesian evidences that are
125 consistent with those from the benchmark retrieval using uncompressed opacity ([Figure 2](#)) within
126 a comparable runtime. The two posterior distributions exhibit slightly different substructure,
127 which we attribute to the compressed results requiring 10% more samples to converge and
128 residual differences between the compressed and uncompressed opacities. The results from
129 this exercise indicate that our compression/decompression scheme is accurate enough to be
130 used in at least some high-resolution retrievals.

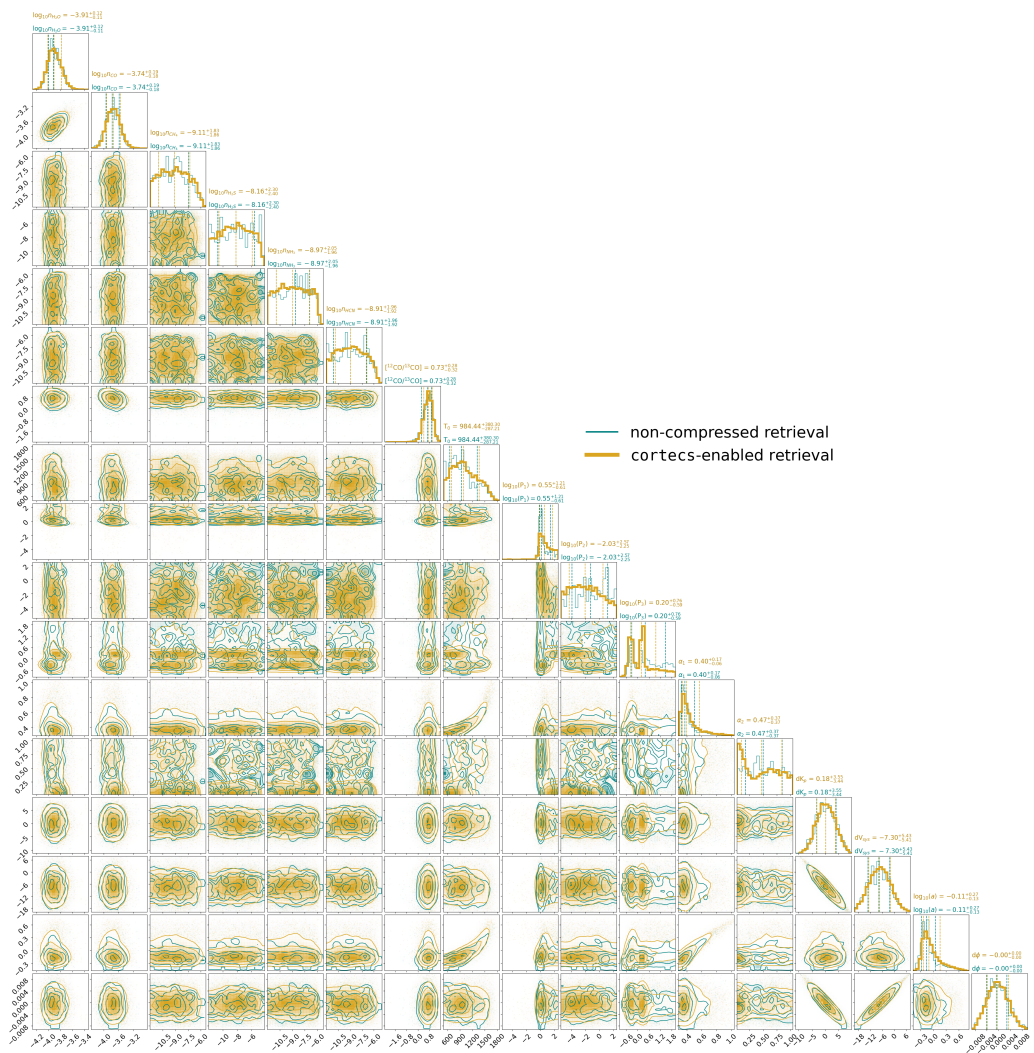


Figure 2: The posterior distributions for our baseline WASP-77Ab retrieval (teal) and our retrieval using opacities compressed by cortecs (gold).

Method	Compression factor	Median absolute deviation	Compression time (s)	Decompression time (s)
PCA	13	0.30	2.6×10^1	2.3×10^2
Polynomials	44	0.24	7.8×10^2	3.6×10^3
Neural network	9	2.6	1.4×10^7	3.6×10^4

¹³¹ Comparison of compression methods used for the HITEMP CO line list (Rothman et al., 2010)
¹³² over the IGRINS wavelength range at a resolving power of 250,000. Note that the neural
¹³³ network compression performance and timings are only assessed at a single wavelength point
¹³⁴ and extrapolated over the full wavelength range.

Acknowledgements

¹³⁵ A.B.S. and E.M-R.K. acknowledge support from the Heising-Simons Foundation. We thank
¹³⁶ Max Isi for helpful discussions.
¹³⁷

References

- 138
- 139 Alzubaidi, L., Zhang, J., Humaidi, A. J., Al-Dujaili, A., Duan, Y., Al-Shamma, O., Santamaría,
140 J., Fadhel, M. A., Al-Amidie, M., & Farhan, L. (2021). Review of deep learning: Concepts,
141 CNN architectures, challenges, applications, future directions. *Journal of Big Data*, 8, 1–74.
142 <https://doi.org/10.1186/s40537-021-00444-8>
- 143 August, P. C., Bean, J. L., Zhang, M., Lunine, J., Xue, Q., Line, M., & Smith, P. C. B.
144 (2023). Confirmation of Subsolar Metallicity for WASP-77Ab from JWST Thermal Emission
145 Spectroscopy. 953(2), L24. <https://doi.org/10.3847/2041-8213/ace828>
- 146 Azzam, A. A., Tennyson, J., Yurchenko, S. N., & Naumenko, O. V. (2016). ExoMol molecular
147 line lists—XVI. The rotation–vibration spectrum of hot H₂S. *Monthly Notices of the Royal
148 Astronomical Society*, 460(4), 4063–4074. <https://doi.org/10.1093/mnras/stw1133>
- 149 Barber, R., Strange, J., Hill, C., Polyansky, O., Mellau, G. C., Yurchenko, S., & Tennyson,
150 J. (2014). ExoMol line lists—III. An improved hot rotation–vibration line list for HCN and
151 HNC. *Monthly Notices of the Royal Astronomical Society*, 437(2), 1828–1835. <https://doi.org/10.1093/mnras/stt2011>
- 153 Beltz, H., Rauscher, E., Kempton, E. M.-R., Malsky, I., & Savel, A. B. (2023). Magnetic
154 effects and 3D structure in theoretical high-resolution transmission spectra of ultrahot
155 jupiters: The case of WASP-76b. *The Astronomical Journal*, 165(6), 257. <https://doi.org/10.3847/1538-3881/acd24d>
- 157 Bradbury, J., Frostig, R., Hawkins, P., Johnson, M. J., Leary, C., Maclaurin, D., Necula, G.,
158 Paszke, A., VanderPlas, J., Wanderman-Milne, S., & Zhang, Q. (2018). JAX: Composable
159 transformations of Python+NumPy programs (Version 0.3.13). <http://github.com/google/jax>
- 161 Buchner, J., Georgakakis, A., Nandra, K., Hsu, L., Rangel, C., Brightman, M., Merloni, A.,
162 Salvato, M., Donley, J., & Kocevski, D. (2014). X-ray spectral modelling of the AGN
163 obscuring region in the CDFS: Bayesian model selection and catalogue. *Astronomy &
164 Astrophysics*, 564, A125. <https://doi.org/10.1051/0004-6361/201322971>
- 165 Chollet, F., & others. (2015). Keras. <https://keras.io>.
- 166 Coles, P. A., Yurchenko, S. N., & Tennyson, J. (2019). ExoMol molecular line lists—XXXV. A
167 rotation–vibration line list for hot ammonia. *Monthly Notices of the Royal Astronomical
168 Society*, 490(4), 4638–4647. <https://doi.org/10.1093/mnras/stz2778>
- 169 Foreman-Mackey, D. (2016). Corner.py: Scatterplot matrices in python. *The Journal of Open
170 Source Software*, 1(2), 24. <https://doi.org/10.21105/joss.00024>
- 171 Gandhi, S., Kesseli, A., Zhang, Y., Louca, A., Snellen, I., Brogi, M., Miguel, Y., Casasayas-
172 Barris, N., Pelletier, S., Landman, R., & others. (2023). Retrieval survey of metals in six
173 ultrahot jupiters: Trends in chemistry, rain-out, ionization, and atmospheric dynamics. *The
174 Astronomical Journal*, 165(6), 242. <https://doi.org/10.3847/1538-3881/accd65>
- 175 Gordon, I. E., Rothman, L. S., Hill, C., Kochanov, R. V., Tan, Y., Bernath, P. F., Birk, M.,
176 Boudon, V., Campargue, A., Chance, K., & others. (2017). The HITRAN2016 molecular
177 spectroscopic database. *Journal of Quantitative Spectroscopy and Radiative Transfer*, 203,
178 3–69. <https://doi.org/10.1016/j.jqsrt.2017.06.038>
- 179 Hargreaves, R. J., Gordon, I. E., Rey, M., Nikitin, A. V., Tyuterev, V. G., Kochanov, R.
180 V., & Rothman, L. S. (2020). An accurate, extensive, and practical line list of methane
181 for the HITEMP database. *The Astrophysical Journal Supplement Series*, 247(2), 55.
182 <https://doi.org/10.3847/1538-4365/ab7a1a>
- 183 Ito, Y., Matsumiya, R., & Endo, T. (2017). Ooc_cuDNN: Accommodating convolutional
184 neural networks over GPU memory capacity. *2017 IEEE International Conference on Big*

- 185 *Data (Big Data)*, 183–192. <https://doi.org/10.1109/BigData.2017.8257926>
- 186 Jolliffe, I. T., & Cadima, J. (2016). Principal component analysis: A review and recent
187 developments. *Philosophical Transactions of the Royal Society A: Mathematical, Physical
188 and Engineering Sciences*, 374(2065), 20150202. <https://doi.org/10.1098/rsta.2015.0202>
- 189 Karman, T., Gordon, I. E., Der Avoird, A. van, Baranov, Y. I., Boulet, C., Drouin, B.
190 J., Groenenboom, G. C., Gustafsson, M., Hartmann, J.-M., Kurucz, R. L., & others.
191 (2019). Update of the HITRAN collision-induced absorption section. *Icarus*, 328, 160–175.
192 <https://doi.org/10.1016/j.icarus.2019.02.034>
- 193 Lee, E. K., Wardenier, J. P., Prinoth, B., Parmentier, V., Grimm, S. L., Baeyens, R., Carone,
194 L., Christie, D., Deitrick, R., Kitzmann, D., & others. (2022). 3D radiative transfer for
195 exoplanet atmospheres. gCMCRT: A GPU-accelerated MCRT code. *The Astrophysical
196 Journal*, 929(2), 180. <https://doi.org/10.3847/1538-4357/ac61d6>
- 197 Line, M. R., Brogi, M., Bean, J. L., Gandhi, S., Zalesky, J., Parmentier, V., Smith, P.,
198 Mace, G. N., Mansfield, M., Kempton, E. M.-R., & others. (2021). A solar c/o and
199 sub-solar metallicity in a hot jupiter atmosphere. *Nature*, 598(7882), 580–584. <https://doi.org/10.1038/s41586-021-03912-6>
- 200 Line, M. R., Wolf, A. S., Zhang, X., Knutson, H., Kammer, J. A., Ellison, E., Deroo, P., Crisp,
201 D., & Yung, Y. L. (2013). A systematic retrieval analysis of secondary eclipse spectra. I. A
202 comparison of atmospheric retrieval techniques. *The Astrophysical Journal*, 775(2), 137.
203 <https://doi.org/10.1088/0004-637X/775/2/137>
- 204 Mace, G., Sokal, K., Lee, J.-J., Oh, H., Park, C., Lee, H., Good, J., MacQueen, P., Oh, J.,
205 S., Kaplan, K., & others. (2018). IGRINS at the discovery channel telescope and gemini
206 south. *Ground-Based and Airborne Instrumentation for Astronomy VII*, 10702, 204–221.
207 <https://doi.org/10.1117/12.2312345>
- 208 Madhusudhan, N., & Seager, S. (2009). A temperature and abundance retrieval method for
209 exoplanet atmospheres. *The Astrophysical Journal*, 707(1), 24. <https://doi.org/10.1088/0004-637X/707/1/24>
- 210 Maguire, C., Gibson, N. P., Nugroho, S. K., Ramkumar, S., Fortune, M., Merritt, S. R., &
211 Mooij, E. de. (2023). High-resolution atmospheric retrievals of WASP-121b transmission
212 spectroscopy with ESPRESSO: Consistent relative abundance constraints across multiple
213 epochs and instruments. *Monthly Notices of the Royal Astronomical Society*, 519(1),
214 1030–1048. <https://doi.org/10.1093/mnras/stac3388>
- 215 Mansfield, M., Wiser, L., Stevenson, K. B., Smith, P., Line, M. R., Bean, J. L., Fortney, J.
216 J., Parmentier, V., Kempton, E. M.-R., Arcangeli, J., & others. (2022). Confirmation
217 of water absorption in the thermal emission spectrum of the hot jupiter WASP-77Ab
218 with HST/WFC3. *The Astronomical Journal*, 163(6), 261. <https://doi.org/10.3847/1538-3881/ac658f>
- 219 Pepe, F., Cristiani, S., Rebolo, R., Santos, N., Dekker, H., Cabral, A., Di Marcantonio,
220 P., Figueira, P., Curto, G. L., Lovis, C., & others. (2021). ESPRESSO at VLT-on-sky
221 performance and first results. *Astronomy & Astrophysics*, 645, A96. <https://doi.org/10.1051/0004-6361/202038306>
- 222 Polyansky, O. L., Kyuberis, A. A., Zobov, N. F., Tennyson, J., Yurchenko, S. N., & Lodi,
223 L. (2018). ExoMol molecular line lists XXX: A complete high-accuracy line list for
224 water. *Monthly Notices of the Royal Astronomical Society*, 480(2), 2597–2608. <https://doi.org/10.1093/mnras/sty1877>
- 225 Prinoth, B., Hoeijmakers, H. J., Pelletier, S., Kitzmann, D., Morris, B. M., Seifahrt, A.,
226 Kasper, D., Korhonen, H. H., Burheim, M., Bean, J. L., Benneke, B., Borsato, N.
227 W., Brady, M., Grimm, S. L., Luque, R., Stürmer, J., & Thorsbro, B. (2023). Time-
228

- 233 resolved transmission spectroscopy of the ultra-hot Jupiter WASP-189 b. 678, A182.
234 <https://doi.org/10.1051/0004-6361/202347262>
- 235 Rothman, L. S., Gordon, I., Barber, R., Dothe, H., Gamache, R. R., Goldman, A., Perevalov,
236 V., Tashkun, S., & Tennyson, J. (2010). HITRAN, the high-temperature molecular
237 spectroscopic database. *Journal of Quantitative Spectroscopy and Radiative Transfer*,
238 111(15), 2139–2150. <https://doi.org/10.1016/j.jqsrt.2010.05.001>
- 239 Savel, A. B., Kempton, E. M.-R., Malik, M., Komacek, T. D., Bean, J. L., May, E. M.,
240 Stevenson, K. B., Mansfield, M., & Rauscher, E. (2022). No umbrella needed: Confronting
241 the hypothesis of iron rain on WASP-76b with post-processed general circulation models.
242 *The Astrophysical Journal*, 926(1), 85. <https://doi.org/10.3847/1538-4357/ac423f>
- 243 Seifahrt, A., Bean, J. L., Stürmer, J., Kasper, D., Gers, L., Schwab, C., Zechmeister, M.,
244 Stefánsson, G., Montet, B., Dos Santos, L. A., & others. (2020). On-sky commissioning of
245 MAROON-x: A new precision radial velocity spectrograph for gemini north. *Ground-Based*
246 *and Airborne Instrumentation for Astronomy VIII*, 11447, 305–325. <https://doi.org/10.1117/12.2561564>
- 248 Tennyson, J., Yurchenko, S. N., Al-Refaie, A. F., Barton, E. J., Chubb, K. L., Coles, P.
249 A., Diamantopoulou, S., Gorman, M. N., Hill, C., Lam, A. Z., & others. (2016). The
250 ExoMol database: Molecular line lists for exoplanet and other hot atmospheres. *Journal of*
251 *Molecular Spectroscopy*, 327, 73–94. <https://doi.org/10.1016/j.jms.2016.05.002>
- 252 Wardenier, J. P., Parmentier, V., Line, M. R., & Lee, E. K. H. (2023). Modelling the effect
253 of 3D temperature and chemistry on the cross-correlation signal of transiting ultra-hot
254 Jupiters: a study of five chemical species on WASP-76b. *Monthly Notices of the Royal*
255 *Astronomical Society*, 525(4), 4942–4961. <https://doi.org/10.1093/mnras/stad2586>